An anti-mycobacterial conjugated oligoelectrolyte effective against *Mycobacterium abscessus*

Short title: A conjugated oligoelectrolyte effective against *Mycobacterium abscessus*

Kaixi Zhang [1]†, Jakkarin Limwongyut [1,2], Alex S. Moreland [2], Samuel Chan Jun Wei [1], Tania Jim Jia Min[1], Yan Sun[3], Sung Jae Shin[4], Su-Young Kim [5], Byung Woo Jhun [5], Kevin Pethe [3,6,7]*, Guillermo C. Bazan [1,2,6,8]*

[1]Department of Chemistry, National University of Singapore, 4 Science Drive 2, 117543 Singapore, Singapore.
[2]Center for Polymers and Organic Solids, Department of Chemistry and Biochemistry, University of California, Santa Barbara, Santa Barbara, CA 93106, USA.
[3]Lee Kong Chian School of Medicine, Nanyang Technological University, 59 Nanyang Drive, 636921 Singapore, Singapore.
[4]Department of Microbiology, Graduate School of Medical Science, Brain Korea 21 Project, Yonsei University College of Medicine, Seoul 03722, South Korea.
[5]Division of Pulmonary and Critical Care Medicine, Department of Medicine, Samsung Medical Center, Sungkyunkwan University School of Medicine, Seoul 06351, South Korea.
[6]Singapore Centre on Environmental Life Sciences Engineering (SCELSE), 60 Nanyang Drive, 639798 Singapore, Singapore.
[7]National Centre for Infectious Diseases (NCID), 16 Jalan Tan Tock Seng, 308442 Singapore, Singapore.
[8]Institute for Functional Intelligent Materials (I-FIM), National University of Singapore, 117544 Singapore, Singapore.

*Corresponding author. Email: kevin.pethe@ntu.edu.sg (K.P.); chmbgc@nus.edu.sg (G.B.)
†Present address: Antimicrobial Resistance Interdisciplinary Research Group, Singapore-MIT Alliance for Research and Technology Centre, Singapore 138602, Singapore.

Abstract

Infections caused by nontuberculous mycobacteria have increased more than 50% in the past two decades and more than doubled in the elderly population. *Mycobacterium abscessus* (Mab), one of the most prevalent of these rapidly growing species, is intrinsically resistant to numerous antibiotics. Current standard-of-care treatments are not satisfactory, with high failure rate and notable adverse effects. We report here a potent anti-Mab compound from the flexible molecular framework afforded by conjugated oligoelectrolytes (COEs). A screen of structurally diverse, noncytotoxic COEs identified lead compound COE-PNH_2, which was bactericidal against replicating, nonreplicating persisters and intracellular Mab.COE-PNH_2 had low propensity for resistance development, with a frequency of resistance below 1.25×10^{-9} and showed no detectable resistance upon serial passaging. Mechanism of action studies were in line with COE-PNH_2 affecting the physical and functional integrity of the bacterial envelope and disrupting the mycomembrane and associated essential bioenergetic pathways. Moreover, COE-PNH_2 was well-tolerated and efficacious in a mouse model of Mab lung infection. This study highlights desirable in vitro and in vivo potency and safety index of this COE structure, which represents a promising anti-mycobacterial to tackle an unmet medical need.

Teaser

We developed a conjugated oligoelectrolyte antibiotic candidate to treat *Mycobacterium abscessus* infection.

Editor's summary

Nontuberculous mycobacteria cause substantial infective burden and can be difficult to treat using current regimens. Zhang *et al*. show that a conjugated oligoelectrolyte, whose structure is unrelated to current antibiotics, was bactericidal against both replicating and nonreplicating *M. abscessus*. The compound was also effective against intracellular infection. Treatment of a mouse lung infection model was efficacious with no signs of toxicity and low resistance development, illustrating the molecule's therapeutic potential. —Catherine Charneski

INTRODUCTION

Nontuberculous mycobacteria (NTM) infections are increasing globally (*1*). NTM lung disease (NTM-LD) is the most common clinical manifestation, with reported annual increases ranging from ~3% in Europe to 15% in Asia (*2*). One also finds that the incidence and prevalence of NTM-LD in the United States have now surpassed that of tuberculosis (*3*). Patients with chronic lung

diseases such as bronchiectasis, chronic obstructive pulmonary disease (COPD), and cystic fibrosis (CF) have a particularly high risk for NTM-LD (*4*). *Mycobacterium avium* complex and *Mycobacterium abscessus* (Mab) complex are most frequently associated with NTM-LD. Notably, Mab remains one of the most difficult-to-treat pathogens among all NTM species (*5*, *6*). The prevalence of Mab in NTM-LD ranges from 5 to 40% across different locations (*7*). Patients with underlying comorbidities such as COPD and CF experience substantial deterioration in lung function, diminished quality of life, and reduced survival rates (*8–10*). This burden is coupled with substantial public health costs and financial hardship (*11*, *12*).

Mab is characterized by an unusually thick and impermeable cell envelope and a set of robust pathways from evolutionary adaptation to hostile environments (*6*). This combination of features endows intrinsic and acquired resistance toward antiseptics and antibiotics (*13*). Furthermore, the ability of NTM to inhabit water systems and to become easily aerosolized, such as in shower droplets, further exacerbates the danger of exposure for vulnerable populations (*14*, *15*). Mab infection is thus a considerable clinical challenge (*16*, *17*). Treatment against Mab is complicated by the lack of bactericidal potency of first-line antibiotics (*18*), the ability to persist in physiologically relevant nutrient-deprived and/or hypoxic microenvironments (*19*), and intracellular residence in phagocytic cells (*20*). Mab infections are therefore recalcitrant to antibiotic treatment, giving rise to empirical standard-of-care treatments that typically involve at least three antibiotic combinations for longer than 12 months (*21*, *22*). Despite the arduous treatment regimen, the cure rate is disappointing, with only 25 to 58% success in culture conversion (*23*). Relapse of infection is often observed, alongside notable adverse side effects secondary to long-term therapy (*24*). The rise in resistance toward first-line antibiotics further exacerbates an already challenging situation, leaving limited therapeutic options (*25*). For example, once macrolide resistance develops, the success rate for culture conversion further drops to 8% (*26*).

Despite the increasing prevalence of Mab and burgeoning antibiotic resistance, the current drug development pipeline is sparse (*23*, *27*), even when compared against *Mycobacterium tuberculosis* (Mtb) (*28*). That the hit rate from antimicrobial compound library screening is extremely low toward Mab (*29*) re-emphasizes the high intrinsic resistance to a broad spectrum of antimicrobials. Research efforts have mainly focused on the development of small molecules and repurposed antituberculosis drugs, which target macromolecular synthetic pathways. However, compounds with a single molecular target are prone to single-step high resistance (*30*). Besides, they are often phenotypically tolerated by quiescent nonreplicating persisters (*31*). Alternative

concepts to develop antibacterial drugs against Mab are therefore worth considering.

Here, we report a small-molecule compound with anti-Mab activity based on the conjugated oligoelectrolyte (COE) platform. Previous studies disclosed structurally diverse COEs that displayed broad spectrum antibacterial activity without being cytotoxic toward eukaryotic cells (*32*, *33*). Through structural optimization and by examining structure-activity relationships, we identified a lead compound that we term COE-PNH_2, which exhibits the most desirable safety and efficacy profile against Mab, both in vitro and in vivo. This study presents a comprehensive report on the in vivo profile of the COE chemical entity, which provides a step forward toward fulfilling a critical gap toward translation for difficult to treat NTM-LD.

RESULTS

COE-PNH_2 is active against Mab and noncytotoxic

COEs are characterized by an electronically delocalized (thus, "π-conjugated") internal hydrophobic segment and pendant hydrophilic side groups bearing cationic charges (fig. S1). COEs have been reported as a chemically tractable framework for developing scaffolds with antimicrobial characteristics (*32*–*34*), and a wide range of structures have been examined to explore structure activity relationships. We recently applied machine-learning techniques to train algorithms capable of predicting COE structures with desirable antimicrobial activity (*35*). Less is known on how the COE structures affect preferential killing of bacteria over mammalian cells (*36*). We thus first screened a range of COE structures and down-selected structurally diverse examples with good cytotoxicity profiles, that is, with 50% inhibitory concentration (IC_{50}) > 128 μg/ml (fig. S1 and table S1). These COE molecules demonstrate diversity in the nature of the cationic group, number of cationic charges, position of charges on side chains, length of pendant hydrocarbon chains, and hydrogen-bonding capabilities (table S1). We further determined minimal inhibitory concentrations (MICs) against Mab American Type Culture Collection (ATCC) 19977, a strain commonly used for anti-Mab drug discovery (*37*). COE-PNH_2 demonstrated the most balanced profile and was selected for further evaluation. The synthetic scheme and structural characterization of COE-PNH_2 can be found in fig. S2.

COE-PNH_2 shows antibacterial activity characterized by an MIC_{90} value of 32 μg/ml (26 μM). Notably, the amine groups at the terminal of each side chain of COE-PNH_2 promote a solubility in aqueous media of >100 mg/ml and may be implicated in hydrogen bonding, a feature that has modulated potency and safety margin in other COEs (*36*). We further probed the activity of COE-

PNH_2 against a panel of clinical isolates and determined efficacy against both rough and smooth Mab isolates, some of which were resistant to first-line antibiotics (Table 1). COE-PNH_2 was compatible with mammalian cells (table S2), with an IC_{50} of 3447 μg/ml against HepG2 cells, giving a selectivity index (IC_{50}/MIC_{90}) of more than 100. Furthermore, COE-PNH_2 was nonhemolytic to red blood cells, with less than 10% hemolysis at 10,000 μg/ml, the highest concentration that was tested (table S2).

Table 1. In vitro activity against *Mycobacterium abscessus* wild-type ATCC 19977 and a panel of clinical isolates.
The lead compound COE-PNH_2 and first-line antibiotics were tested. WT, wild type; UC, upper lobe cavity; NB, nodular bronchiectasis. AMK, amikacin; CLR, clarithromycin; LZD, linezolid. Units: μg/ml. $MBC_{99.9}$, the minimal bactericidal concentration that eradicates 99.9% of bacteria.

Strains		Morphotype	COE-PNH_2	AMK	CLR	LZD
WT	MIC_{90}	Smooth	32	16	2	8
	$MBC_{99.9}$	Smooth	64	>128	>32	>128
Clinical isolates MIC_{90}	UC17	Rough	32	16	16	8
	UC18	Smooth	32	32	2	>128
	NB19	Rough	64	32	8	32
	NB20	Smooth	32	32	4	>128
	UC23	Rough	32	64	>128	4
	NB25	Smooth	32	128	>128	64

Of additional interest, COE-PNH$_2$ also demonstrated potency against other bacterial strains commonly identified from patients with COPD and CF, including Gram positives, Gram negatives, and mycobacteria (table S3). Such activity may offer additional benefits to patients with Mab, who often have comorbidities in the lungs and are susceptible to exacerbation by bacterial infections.

COE-PNH$_2$ is bactericidal, kills persisters, and is efficacious in whole blood

Kill-kinetics experiments were conducted to evaluate the bactericidal activity of COE-PNH$_2$ (Fig. 1A). These studies revealed that at 1× MIC, COE-PNH$_2$ exhibited bacteriostatic activity. However, at 2× MIC, a 4 $\log_{10}$ reduction of colony-forming units (CFUs) was observed by day 4. Increasing the concentration to 4× MIC led to complete eradication of bacilli by day 3, with CFUs below the limit of detection (<100 CFU/ml). Antibiotic controls amikacin (AMK) and linezolid (LZD) did not eradicate Mab even at concentrations as high as 128 μg/ml (fig. S3). Together, these findings indicate that, although its MIC value is larger relative to comparator antibiotics, COE-PNH$_2$ has superior bactericidal potency compared to AMK, LZD, or clarithromycin (CLR) (Table 1).

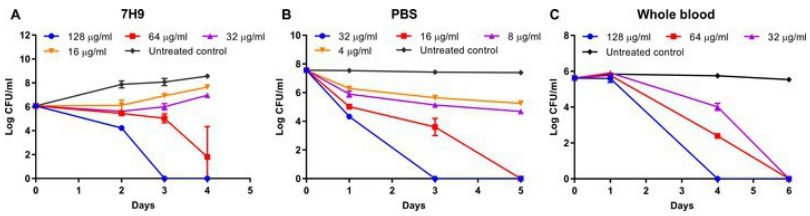

Fig. 1. Kill-kinetics of COE-PNH$_2$ against *Mycobacterium abscessus* ATCC19977 in various media mimicking different microenvironments.
Assays were done in (**A**) nutrient 7H9 broth, (**B**) PBS nutrient starvation, and (**C**) whole blood. Error bars are represented as means ± SD.

A complication with antibiotic treatment is that it can lead to biphasic killing, leaving behind a small percentage of persister bacteria that are phenotypically tolerant (*31*). Such behavior is observed with AMK, where further increases in concentration do not improve killing (fig. S3). The fact that COE-PNH$_2$ eradicates Mab in vitro (Fig. 1A) implies its potential potency against persisters. To evaluate this hypothesis, we tested the potency of COE-PNH$_2$ against nutrient-starved, nonreplicating Mab, which are known for their extreme antibiotic tolerance (*19*). Mab cells were first starved in phosphate-buffered saline (PBS) for 7 days, where no changes in CFU

were observed confirming a nonreplicating quiescent state. COE-PNH_2 at a concentration as low as ½× MIC completely eradicated nutrient-starved persisters (Fig. 1B), indicating that the compound is even more potent against nonreplicating compared to replicating Mab.

Unlike well-defined in vitro culture medium and buffers, physiological environments are more complex, where the activity of many antimicrobials is hindered (*38*, *39*). To verify COE-PNH_2 activity in physiologically relevant conditions, we conducted MIC tests in the presence of human serum albumin (40 g/liter), the most abundant blood protein (*40*). No changes in the MIC or MBC values were observed (table S4), confirming that antimicrobial activity was not affected by plasma protein. We further conducted kill-kinetics in whole blood (Fig. 1C) to account for the presence of high concentrations of interfering substances such as degrading enzymes, divalent salts, and anionic proteins (*41*). COE-PNH_2 retained bactericidal activity and resulted in >5 $\log_{10}$ CFU reduction at 1× MIC. Altogether, COE-PNH_2 kill-kinetic assays in different media, namely, growth medium, nutrient-deprived buffer, and blood, confirmed the robustness of its bactericidal activity.

COE-PNH_2 is active against intracellular Mab

In addition to its extracellular lifestyle, Mab can invade phagocytic cells and persist intracellularly (*20*). Many first-line antibiotics, such as AMK, have limited penetration into mammalian cells and therefore experience reduced access to intracellular Mab (*42*). It has recently been shown that COEs are capable of penetrating mammalian cells such as A549 lung epithelium cells (*43*, *44*). An absorption assay confirmed the uptake of COE-PNH_2 into THP-1 macrophages (fig. S4). These considerations motivated us to test the activity of COE-PNH_2 against intracellular Mab inside macrophages. In an in vitro THP-1 intracellular infection model, COE-PNH_2 inhibited the growth of intracellular bacilli at 1× MIC. On day 3, a 1.4 $\log_{10}$ CFU difference was observed compared with untreated controls. At 2× MIC, COE-PNH_2 killed intracellular Mab, with 1.0 and 2.4 $\log_{10}$ CFU reduction compared with baseline and untreated control, respectively (Fig. 2). As intracellular mycobacteria are increasingly recognized as a niche for relapse of infection (*5*, *6*), the bactericidal activity of COE-PNH_2 against intracellular Mab has the potential to offer a notable advantage.

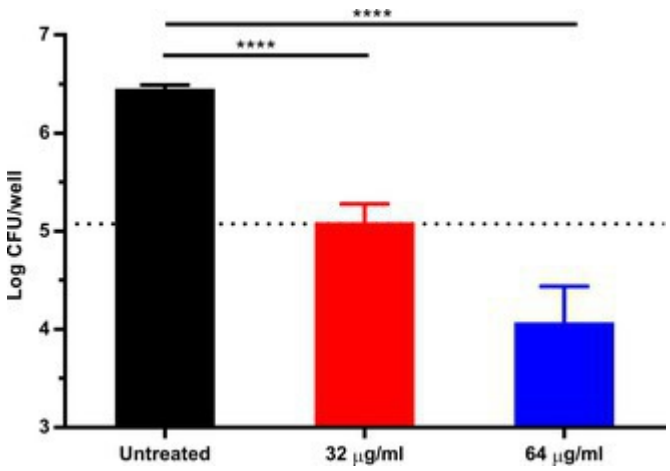

Fig. 2. COE-PNH$_2$ at 1× and 2× MIC kills intracellular *Mycobacterium abscessus* ATCC19977 in vitro, in a THP-1 infection model with treatment duration of 3 days. Dotted line represents the baseline CFU before treatment. Error bars are represented as means ± SD. Statistical significance was analyzed using one-way analysis of variance (ANOVA) followed by Dunnett's test. ****$P < 0.0001$.

Drugs with intracellular penetration are commonly questioned regarding potential damage on the organelles of mammalian cells, with a focus on mitochondrial toxicity (*45*). This is particularly relevant for lipophilic cationic drugs, which can show increased accumulation in the mitochondrial matrix in response to the transmembrane potential across the mitochondrial membrane (*46*). Because mammalian cells grown in galactose medium are more susceptible to mitochondrial toxicity (*47*), we conducted a glucose/galactose assay in different media and compared adenosine 5′-triphosphate (ATP) production. As reported in literature (*48*), we observed that the electron transport chain inhibitors rotenone and oligomycin resulted in markedly reduced ATP production in galactose medium relative to glucose medium (fig. S5, A and B). In contrast, no difference in ATP concentration was observed upon COE-PNH$_2$ treatment, irrespective of the carbon source (fig. S5C). This assay supports the safety of COE-PNH$_2$ and the lack of mitochondrial toxicity in mammalian cells despite its intracellular penetration.

COE-PNH$_2$ has a low propensity for resistance development

Escape mutants to a candidate antibacterial drug are usually selected on agar plates. However, COE-PNH$_2$ binds to negatively charged agar, rendering such tests unreliable. This complication

can be circumvented by replacing agar with neutrally charged agarose. Thus, 8×10^8 CFU Mab were inoculated onto agarose plates containing 4× MIC COE-PNH_2. Multiple attempts to select spontaneous mutants resistant to COE-PNH_2 were unsuccessful, indicating a frequency of resistance (FoR) below 1.25×10^{-9}. Compared to antibiotics and drug candidates in the pipeline with an FoR between 10^{-5} and 10^{-8}, COE-PNH_2 is less prone for resistance development (*49*–*55*). To ensure that the FoR was not affected by changing from agar to agarose, we further conducted the test for comparator antibiotic imipenem (IPM) at 4× MIC on solid media (table S5). The FoR values remained at similar magnitudes regardless of the solidifying agent.

Spontaneous mutant selection mimics the condition in clinical settings where high drug concentrations above MIC are encountered. Another scenario of interest is the emergence of resistance under repeated exposure at subinhibitory concentrations, especially for long-duration treatments (*56*). To mimic this condition, we conducted serial passaging tests where Mab was challenged with a series of step-wise increasing drug concentrations over a period of 14 passages. In contrast to the control AMK, where a 64-fold increase in MIC was observed, passaging with COE-PNH_2 did not modify the initial MIC (Fig. 3). Together, these assays derisk the emergence of resistance toward COE-PNH_2, highlighting another advantage over conventional antibiotics.

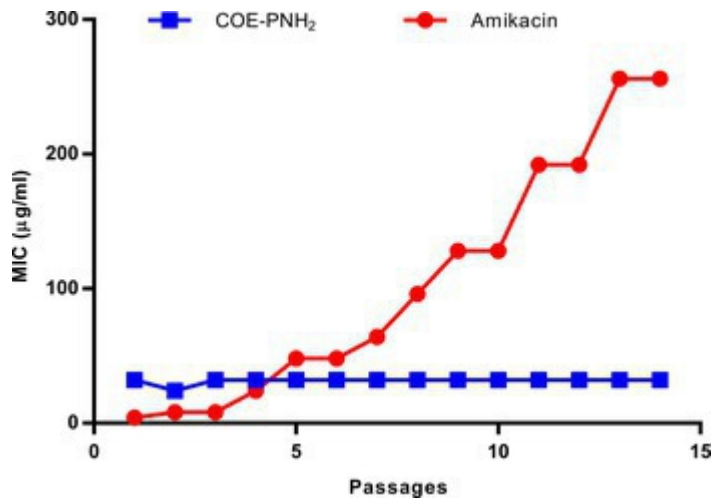

Fig. 3. Serial passaging test for COE-PNH_2 propensity of resistance development. *Mycobacterium abscessus* ATCC19977 was challenged with a series of step-wise, twofold increasing drug concentrations progressively over a period of 14 passages. AMK was used as antibiotic control. MIC, minimal inhibitory concentration.

COE-PNH_2 is membrane active and affects mycomembrane structure and cellular bioenergetics

The hydrophilic-hydrophobic-hydrophilic topology of COE molecules resembles that of the lipid bilayer in biological membranes. The bacterial membrane has been reported as a plausible target for several antimicrobial COEs (*57*). It seemed reasonable that COE-PNH_2 is no exception. To gain insight into the mechanism of action, we used transmission electron microscopy (TEM) to visualize Mab cells after 24-hour COE-PNH_2 treatment. The resulting images show that the untreated control bacilli have an intact cell envelope, with clearly visible mycomembrane, peptidoglycan layer, and cytoplasmic membrane (Fig. 4A). Upon COE-PNH_2 treatment at ½× MIC, a change in the morphology of the outermost surface was observed, possibly due to the interaction with the mycomembrane (Fig. 4B). At 1× MIC, in addition to mycomembrane damage, multiple intracellular vesicles were observed inside the cells (Fig. 4C and fig. S6). These vesicles showed well-defined electron-dense envelopes, implying that they are enclosed by lipid bilayers. Although the detailed stepwise sequence for the formation of such vesicles is not clear, it is reasonable in view of the substantial changes to the cytoplasmic membrane organization to assume that essential membrane functionalities were impaired. Mesh-like electron-dense structures are also observed (fig. S6). At 2× MIC, cells were lysed with a ruptured cell envelope (Fig. 4D), which could be a collective effect of the interruption to both mycomembranes and cytoplasmic membranes.

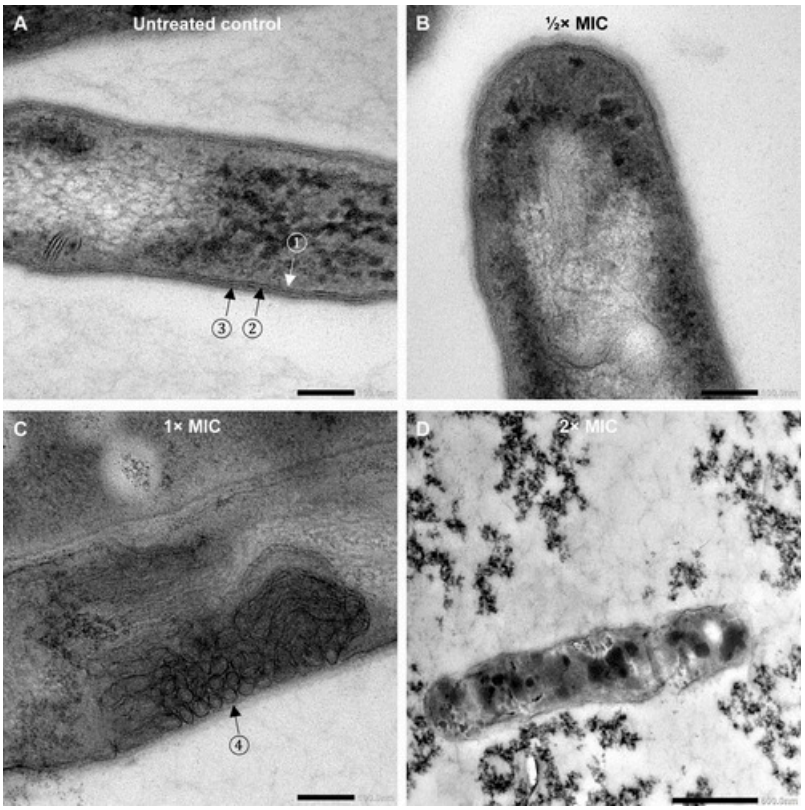

Fig. 4. COE-PNH$_2$ disrupts the integrity of the cell envelope in *Mycobacterium abscessus*. Mab ATCC19977, untreated or treated with an increasing concentration of COE-PNH$_2$, was analyzed by transmission electronic microscopy (TEM). Images revealed (**A**) intact cytoplasmic membranes (arrow ①), cell wall (arrow ②), and mycomembranes (arrow ③) in untreated controls and (**B**) disrupted mycomembranes at ½× MIC. (**C**) Accumulation of intracellular vesicles (arrow ④) and alteration of the physical/functional integrity of cytoplasmic membrane at 1× MIC and (**D**) total cell rupture at 2× MIC. Scale bars, 100 nm (A to C) and 500 nm (D).

The interactions of Mab with adjacent cells (aggregation), or between Mab and surfaces (adhesion), are dictated by the outermost mycomembrane. To confirm the observed effect of COE-PNH$_2$ on mycomembranes, we further conducted aggregation and adhesion assays. In the aggregation assay, Mab in liquid culture was challenged with subinhibitory concentrations of COE-PNH$_2$ under continuous shaking for 24 hours. The untreated control sample remained homogeneously dispersed, whereas COE-PNH$_2$ treatment at ½× MIC led to clumped culture (fig. S7). Quantitative analysis confirmed an increase in the aggregation index upon COE-PNH$_2$

treatment (Fig. 5A). In addition, subinhibitory concentrations of COE-PNH$_2$ promoted the adhesion of Mab cells to a plastic surface in a concentration-dependent manner (Fig. 5B). Both assays confirmed changes in the surface properties of Mab cells, likely attributed to the interaction between COE-PNH$_2$ and the mycomembrane. An intriguing feature of mycomembrane-targeting compounds is possible synergistic effects with antibiotics (*58*). Notably, COE-PNH$_2$ enhanced the activity of first-line antibiotics against Mab. COE-PNH$_2$ demonstrated a synergistic effect with AMK and IPM (fig. S8, A and B) and an additive effect with CLR and LZD (fig. S8, C and D). This finding underscores the potential usage of COE-PNH$_2$ as antibiotic adjuvants against Mab.

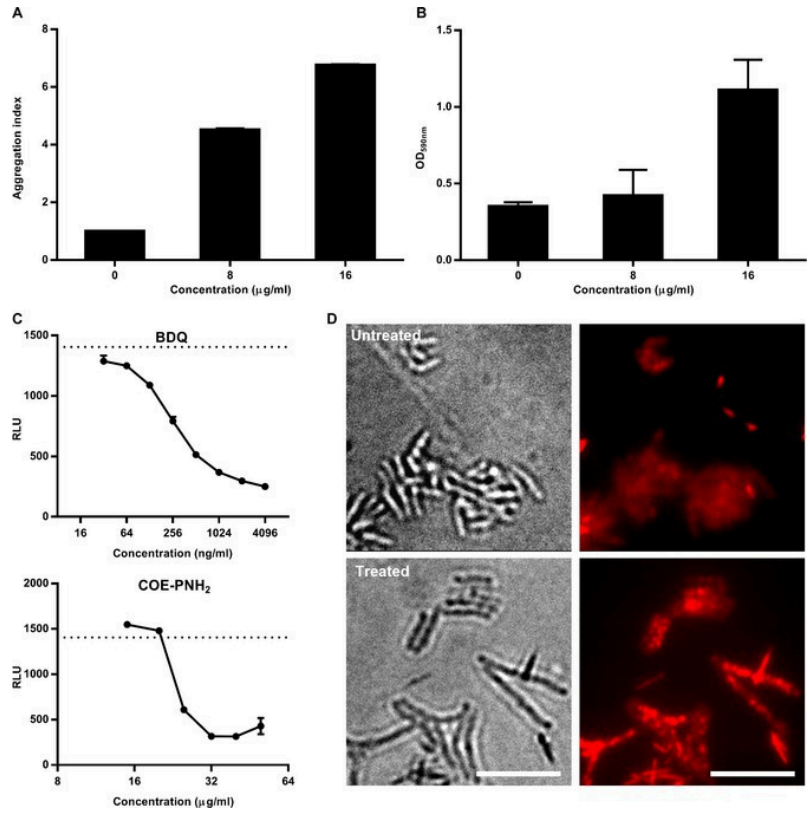

Fig. 5. COE-PNH$_2$ damages the Mab mycomembrane and inhibits the electron transport chain.

(**A**) Aggregability of Mab ATCC19977 was evaluated after treatment with subinhibitory concentrations of COE-PNH$_2$. (**B**) Adhesion for changes in surface property upon treatment with subinhibitory concentrations of COE-PNH$_2$. Adhesive Mab attached to the surface were stained by crystal violet dye. (**C**) COE-PNH$_2$ depleted intracellular ATP in a concentration-

dependent manner. Top: BDQ, bedaquiline positive control; bottom: COE-PNH_2. (**D**) Fluorescent microscope images of intracellular lipid droplets upon treatment of 1× MIC COE-PNH_2. Top panels: untreated control; bottom panels: COE-PNH_2 treated. Lipid droplets were stained by Nile Red dye. Scale bars, 10 μm. Error bars are represented as means ± SD. RLU, relative light unit.

That nonreplicating persisters are more susceptible to COE-PNH_2 recalls an intriguing observation with *M. tuberculosis*: Drugs targeting essential bioenergetics pathways demonstrate improved bactericidal activity against persisters (*59*). This is because under nonreplicating conditions, mycobacteria still need to maintain ATP homeostasis via oxidative phosphorylation. This represents a metabolically weak point and serves as a potential target for drug development. A similar phenomenon has also been reported for Mab (*60*). In line with this background work, bedaquiline is bacteriostatic against nutrient-rich replicating Mab but becomes concentration-dependent bactericidal against nutrient-deprived persisters (fig. S9). We hypothesized that COE-PNH_2 causes disorganization of the cytoplasmic membrane and affects bacterial bioenergetics. Quantification of intracellular ATP showed that COE-PNH_2 induced a concentration-dependent depletion of ATP (Fig. 5C). At 1× MIC, the magnitude of ATP depletion after 5-hour co-incubation was similar to bedaquiline control.

We further imaged COE-PNH_2–treated cells by fluorescent microscopy. Mab cells were treated with COE-PNH_2 at 1× MIC for 5 hours, a condition that confirmed ATP depletion. Compared to the actively multiplying Mab control, COE-PNH_2 treatment led to accumulation of intracellular lipid inclusions (ILIs) that were stained by Nile Red (Fig. 5D and fig. S10, A and B) (*61*). Bacterial elongation (fig. S10C), increase in Nile Red fluorescence intensity (fig. S10D), and alteration in single-bacillary fluorescence distribution patterns (fig. S10E) were observed in COE-PNH_2–treated cells. To further elucidate the ultrastructural features of ILIs, these ATP-depleted Mab cells were also imaged by TEM (fig. S11). Mab displayed four types of ILI profiles based on the number and size of ILIs, as previously described (*62*). In the untreated control sample of actively multiplying bacilli (fig. S11A), most Mab cells demonstrated an ILI^{-} profile with no lipid droplets (left image); very few cells displayed an ILI^{1+} profile with one to two ILIs of diameter < 0.1 μm (right image). The COE-PNH_2–treated sample exhibited notably different ILI profiles (fig. S11B): Many cells displayed an ILI^{2+} profile with several ILI of 0.2 to 0.3 μm in diameter (left image); some cells also displayed an ILI^{3+} profile with multiple ILIs of 0.3 to 0.5

μm in diameter that occupied most of the mycobacterial cytoplasmic space (right image). Quantitative analysis confirmed >90% of COE-PNH_2–treated bacilli had ILIs, in contrast to <5% in untreated control cells (fig. S11C). Together, bacterial elongation and ILI accumulation are typical morphotypic changes of Mab in response to disruption in energy production/supply (*63*).

Collectively, these data suggest that COE-PNH_2 interferes with the Mab envelope and impairs its physical or functional integrity. COE-PNH_2 possibly lodges in both the mycomembrane and the cytoplasmic membrane. The two-pronged action against the mycomembrane and bioenergetics of the cytoplasmic membrane likely accounts for the bactericidal activity and lack of resistance (*64*).

COE-PNH_2 is safe and efficacious in vivo

We proceeded to evaluate the in vivo safety and efficacy of COE-PNH_2 in a mouse model. In the first set of experiments to evaluate safety, single doses of COE-PNH_2 were administered at 10 mg/kg and 20 mg/kg intravenously (i.v.) (fig. S12A), or at 5 mg/kg and 10 mg/kg intranasally (i.n.) (fig. S12B). Mice tolerated both systemic and intranasal deliveries without weight loss. Examination of lung tissues from the intranasal group (10 mg/kg) did not show any notable histological difference compared to the saline vehicle group (table S6). As treatment of NTM-LD involves prolonged usage of antibiotics, we further evaluated the safety of COE-PNH_2 upon repetitive dosing. Mice received daily intravenous injections at 10 mg/kg for seven consecutive days or daily intratracheal instillation at 10 mg/kg for 3 days. No weight loss was observed in both tests (fig. S12, C and D). These results confirmed that COE-PNH_2 is well-tolerated in vivo.

We further tested the in vivo efficacy of COE-PNH_2 in an acute Mab lung infection model. C3HeB/FeJ mice received a daily dexamethasone injection 1-week before infection and throughout the experiment (*65*). Infection was established through intranasal delivery of Mab at day 0. Mice received intratracheal saline vehicle control daily, COE-PNH_2 at 2.5 mg/kg or 5 mg/kg QOD (every other day), or AMK at 5 mg/kg daily. Lung CFUs of the vehicle control group continued to increase over time, indicating the infection progression (Fig. 6A). Of relevance is that the lung CFUs of the AMK group continued to decrease by day 8 but remained unchanged until day 12. In contrast, treatments with COE-PNH_2 led to continued reduction of lung CFUs throughout the experimental period. Specifically, COE-PNH_2 dosed at 5 mg/kg QOD resulted in 2.4 $\log_{10}$ CFU reduction at the end point, superior to AMK control despite AMK being dosed twice as frequently (Fig. 6A and table S7). Acid-fast bacilli staining of the lung organs harvested at day 12 confirmed that much fewer bacilli were present in the COE-PNH_2–treated groups (Fig. 6B).

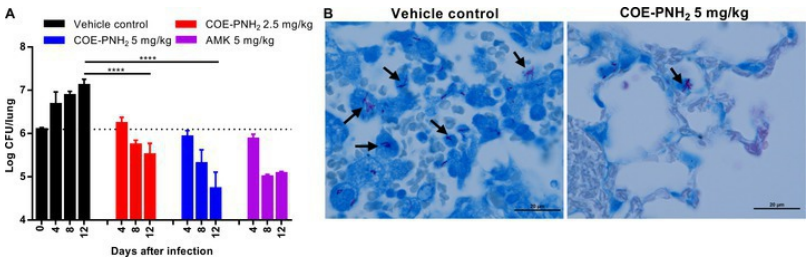

Fig. 6. In vivo efficacy of COE-PNH_2 in an acute mouse Mab lung infection model. (**A**) Bacterial CFU changes in the lungs of C3HeB/FeJ mice treated with vehicle control daily (black), COE-PNH_2 at 2.5 mg/kg (red) or 5 mg/kg (blue) every other day, or AMK control at 5 mg/kg daily (purple). All treatments are administered intratracheally. Error bars are represented as means ± SD. Statistical significance was analyzed using one-way ANOVA followed by Dunnett's test (GraphPad Prism). ****$P < 0.0001$ (**B**) Acid-fast staining of lung samples from vehicle control (left) and COE-PNH_2^- mice (5 mg/kg; right). Arrows indicate acid-fast bacilli.

To check for emergence of resistance at the experimental end point, eight Mab colonies from the plated homogenates of COE-PNH_2–treated groups were randomly selected. The MICs of COE-PNH_2 remain unchanged, confirming the low propensity of resistance development in an in vivo setting. Mice receiving COE-PNH_2 at high doses (5 mg/kg QOD) did not show any adverse clinical signs based on daily observation and no body weight loss (fig. S13).

DISCUSSION

Antibiotic resistance has become a major cause of death, claiming 1.27 million lives directly and 4.95 million lives indirectly in 2019, surpassing those of HIV and malaria (*66*). Antibiotic resistance and tolerance are particularly worrisome in the context of mycobacteria (*64*, *67*). Mab is one of the most antibiotic-resistant mycobacteria with limited therapeutic options (*68*). Mab exhibits numerous mechanisms to survive exposure to antimicrobials, including low permeability, robust drug export systems, genetic polymorphism of targeted genes, and various target-modifying and antibiotic-inactivating enzymes (*17*). Their presence as metabolically inactive persisters and intracellular residence in phagocytes further diminishes the activity of first-line antibiotics. Unfortunately, the optimal drug regimen and duration for Mab infection is not known, and the current regimens is largely empirical and lack proven or predictable efficacy (*28*). Suggested

therapy by the British Thoracic Society and American Thoracic Society and the Infectious Diseases Society of America consists of two phases that usually spans 18 to 24 months. It includes an initial intense phase for least 4 weeks, with a macrolide, parenteral AMK, and at least one additional antibiotic such as tigecycline, IPM, or cefoxitin. The subsequent continuation phase lasts for at least 12 months and involves a macrolide, inhaled AMK, and at least two additional oral antibiotics such as clofazimine, LZD, or minocycline. Despite aggressive usage of antibiotics, more than half of the patients do not achieve sputum conversion (*69*), yet more than 70% of the patients suffer from notable adverse side effects (*24*). Additional therapeutic concepts are urgently needed to tackle this "incurable nightmare" (*24*).

The mycobacterial envelope has received interest as a viable therapeutic target (*70*). A functionally intact membrane is essential for both actively replicating bacteria and quiescent persisters (*71*). Compounds targeting bacterial membrane, through physical disruption or interference with essential membrane functionalities, often lead to rapid bactericidal activity regardless of the metabolic state of the bacteria. This has been demonstrated in the field of Mtb research and very recently in Mab (*71*). Several drug candidates, such as indole-2-carboxamides and piperidinol derivatives, target the essential mycolic acid transporter MmpL3 and eventually lead to impaired cell wall and cell death (*28*). A few MmpL3 inhibitors have demonstrated moderate bactericidal activity (assessed by MBC_{90}) against nonreplicating Mab persisters (*19*). However, these molecules target a specific enzyme, and spontaneous mutants are readily identified with a relatively high frequency. The COE molecule used in this study, namely, COE-PNH_2, which targets the physical and functional integrity of the bacterial envelope rather than specific enzymes, demonstrated a lower frequency of spontaneous mutation and resistance evolution. Its bactericidal activity against replicating, nonreplicating persisters, and intracellular Mab further ensues comprehensive eradication of bacteria, without leaving behind a niche for relapse of infection.

Membrane-disrupting compounds, exemplified by antimicrobial peptides (AMPs), are often cationic amphiphiles (*72*). The physical interaction with bacterial membrane also leads to rapid bactericidal activity and low propensity of resistance development. However, because of their amphiphilic nature, they often display indiscriminate toxicity to mammalian cells and erythrocytes. COE-PNH_2 is noncytotoxic, allowing excellent bio- and hemocompatibility. The HC_{10} value is greater than 10,000 μg/ml, far exceeding its effective concentration required to eradicate bacteria. Conventional cationic amphiphilic antimicrobials are also sensitive to confounding factors in complex physiological environments due to the presence of excessive anionic or hydrophobic components. The robust bactericidal activity of COE-PNH_2 in complex conditions underlines

another important feature of this chemical entity.

Selectivity toward bacteria can be achieved through informed design of COE molecules capable of differentiating between bacteria and mammalian cell membranes. These differences encompass attributes such as charge, hydrophobicity, fluidity, composition, and specific membrane components. In previous studies, we examined a homologous series of COEs and identified scaffolds with optimum charge-to-charge, charge-to-core, and core lengths (*33*, *34*); we also used machine-learning techniques to identify the essential elements in the molecular structure that most strongly correlate with antimicrobial activity (*35*); our subsequent study of COEs with amide side chains highlights hydrogen bonding as an important modulator for bacterial targeting and hints at more subtle interactions between bacterial membrane and COEs (*36*).

Prior studies on COE antimicrobial development have mainly focused on the molecular design and structural iterations to modulate in vitro efficacy. Little has been reported to demonstrate in vivo activities. A prior study reported that COE2-2hexyl successfully rescued mice infected with methicillin-resistant *Staphylococcus aureus* or *Klebsiella pneumoniae* in a sepsis model (*73*). However, COE2-2hexyl exhibits detectable cytotoxicity to mammalian cells (IC_{50} < 20 μg/ml). Our study comprehensively demonstrates a large therapeutic window for COE-PNH_2, both in vitro and in vivo, and highlights the flexibility of the COE platform to generate derivatives with improved properties. Particularly interesting is that energy depletion can be specifically achieved in Mab, without affecting mammalian mitochondria.

As COE is a relatively new antibiotic platform, a limitation of our study is that we lack a comprehensive mechanism of action. At a molecular level, the interaction between COE-PNH_2 and mammalian and bacterial envelopes across different strains remains to be further elucidated. Besides targeting bioenergetics, to what extent the interaction with the mycomembrane contributes to the enhanced potency against nutrient-starved persisters remains uncertain. It is also unclear if the hydrogen-bonding moieties of COE-PNH_2 contribute to the much-improved safety profile. Further toxicity studies await. The origin of the intracellular vesicles in Mab treated with COE-PNH_2 also remains poorly understood. They might be extracellular vesicles that were faultily accumulated within the membrane due to interrupted bioenergetics, or reformed microstructures because of physical interactions between COE-PNH_2 and the cytoplasmic membrane lipids. The pathways involved in the penetration of COE-PNH_2 into mammalian cells and intracellular killing toward Mab are intriguing too. Answering these questions will be important to further guide molecular design in the continued optimization of the COE scaffold.

In summary, we have developed a safe and efficacious small-molecule drug against Mab based on the COE platform. The lead compound COE-PNH_2 demonstrates high potency toward Mab and an improved safety margin over previously studied COEs. It targets the integrity of bacterial envelope, affecting both mycomembrane and bioenergetic functionality of the cytoplasmic membrane. This two-pronged action endows its low propensity of resistance development and robust bactericidal activity against both replicating and nonreplicating persisters. COE-PNH_2 is well-tolerated in vivo with proven efficacy in a mouse acute lung infection model. This study highlights the therapeutic potential of membrane-targeting COEs as potent anti-Mab candidates.

MATERIALS AND METHODS

Study design

The objectives of this study were to evaluate the therapeutic potential of the flexible molecular framework of COEs against Mab. In vitro screening of structurally diverse COE structures identified the lead molecule, COE-PNH_2 with low cytotoxicity and good antimicrobial activity against the type strain Mab ATCC 19977. Further clinically relevant in vitro assays were performed to assess its bactericidal activity, resistance propensity, intracellular-killing efficacy, and preliminary mechanism of action. Additional profiling on its biocompatibility toward various mammalian cell lines and mitochondria was conducted. In vivo safety of single dosing and repetitive dosing in mice were assessed. Last, in vivo efficacy was evaluated in an acute Mab mouse lung infection model. All in vitro experiments were repeated at least two times, with ≥2 biological replicates each time. All in vivo procedures were reviewed and approved by the Institutional Animal Care and Use Committee (IACUC) of National University of Singapore.

Materials

Antimicrobial COEs were synthesized in the laboratory following the procedures in the Supplementary Materials. All chemicals and antibiotics were purchased from Sigma-Aldrich except bedaquiline that was purchased from MedChemExpress.

Strains, cell lines, and culture media

Mab ATCC 19977 (smooth morphotype) were purchased from ATCC. Clinical Mab strains were isolated from patients at the Samsung Medical Centre, Seoul South Korea (*74*). Bacteria was cultured at 37°C in Middlebrook 7H9 liquid medium supplemented with 0.2% glycerol, 0.05%

Tween 80, and 10% albumin-dextrose-catalase (ADC) (referred to as 7H9t). For CFU enumeration, bacteria were plated on Middlebrook 7H10 or 7H11 agar supplemented with 10% oleic acid ADC (OADC). For test under nutrient-starvation condition, Mab was grown in 7H9t to log phase, washed three times in PBS with 0.025% Tween 80 (PBSt), and maintained in PBSt at 37°C for 7 days. *Mycobacterium bovis* and *Mycobacterium smegmatis* were cultured at 37°C in 7H9t. Gram-positive and Gram-negative bacteria were obtained from ATCC or Collection de l'Institut Pasteur and grown in cationic-adjusted Mueller Hinton broth at 37°C. Mammalian cell lines were purchased from ATCC and maintained at 37°C, 5% CO_2. HepG2, 3T3, and A549 cell lines were maintained in Dulbecco's modified Eagle's medium supplemented with 10% fetal bovine serum (FBS). THP-1 cells were maintained in RPMI 1640 supplemented with 10% FBS.

MIC and MBC determination

Log phase Mab ATCC 19977 were adjusted to optical density at 600 nm (OD_{600nm}) of 1.0 in 7H9t. COEs were dissolved at 10 mg/ml in sterile deionized (DI) water. AMK, LZD, and CLR were dissolved at 50 mg/ml in sterile DI water, dimethyl sulfoxide, and acetone, respectively. Testing compounds were further diluted in 7H9t to desired starting concentration and twofold serially diluted in a flat-bottom 96-well plate at a volume of 50 μl. Mab culture was diluted 1:100 in 7H9t, and 50 μl of bacteria culture was added to each well. The 96-well plate was incubated at 37°C for 3 days without agitation. The plate was briefly mixed using a microplate shaker, and the OD_{600nm} absorbance were recorded using a Tecan Plate reader (Infinite 200 Pro). MIC_{90} is defined as the minimal concentration that inhibits 90% growth calculated by OD values.

For minimal bactericidal concentration (MBC) test, the 96-well plate in MIC test was incubated for 5 to 7 days. The bacterial suspension was 10-fold serially diluted in PBSt and plated onto 7H10 agar plates to enumerate bacterial CFUs. $MBC_{99.9}$ is defined as the minimal concentration that kills 99.9% (3 $\log_{10}$ reduction) of the starting bacterial inoculum.

Time-kill assays

For the time-kill assay in nutrient-rich medium, log phase Mab was adjusted to OD_{600nm} 0.5 and diluted 1:100 in 7H9t. Testing compounds were added at desired concentrations and the suspension was incubated at 37°C. At desired time points, 20 μl of the suspension was 10-fold serially diluted and plated onto 7H10 agar plates for CFU enumeration. For nutrient-starved persister assay, 7-day starved Mab cells were used, and a time-kill assay was conducted in PBSt. For Mab in whole blood, log phase Mab was washed three times with PBSt and resuspended to OD_{600nm} of 0.5.

Bacteria was 1:100 diluted in ICR<< Q1 - Query: Please provide the expanded form of “ICR,” if any. Ans: **kevin.pethe@ntu.edu.sg:** There is no expanded form of "ICR". It is a technical term itself. >> mouse blood (InVivos), and a time-kill assay was conducted.

Intracellular infection

The in vitro intracellular infection model was conducted following a published protocol with minor modifications (*75*). THP-1 cells were seeded at 100,000 cells per well in a tissue culture–treated 24-well plate. Phorbol 12-myristate 13-acetate (20 ng/ml) was added to the medium and incubated for 48 hours to differentiate THP-1 macrophages. The supernatant of each well was aspirated, and cells were washed three times with PBS. Log phase Mab were washed three times with PBSt and diluted in RPMI medium at a multiplicity of infection of 10:1. After 1-hour infection, extracellular bacteria were removed by thorough washing with PBS for three times. Intracellular infection was allowed to progress for 24 hours. The cells were washed three times with PBS to remove any escaped extracellular bacteria. COE-PNH_2 in RPMI solution was added at desired concentrations and replenished daily for 3 days. At desired time points, supernatants were discarded, and cells were washed thoroughly with PBS three times and lysed in DI water for 10 min. The suspension was 10-fold serially diluted in PBSt and enumerated on 7H10 agar plates.

Resistance evolution

For serial passaging, COE-PNH_2 or AMK were twofold serially diluted in 7H9t in a 96-well plate. Log phase Mab was added to a final OD_{600nm} of 0.005, and the plate was incubated for 3 to 4 days at 37°C. For the next passage, bacterial suspension in the presence of ½× MIC compound was used as the inoculum. A bacterial suspension of ¼× MIC well was used if the OD_{600nm} of ½× MIC well were too low (<0.25). The test was repeated for 14 passages, and the MIC values of each passage were recorded.

Mechanism of action studies

Log phase Mab cells were adjusted to OD_{600nm} of 0.25 in 10 ml of 7H9t. COE-PNH_2 was added at ½×, 1×, and 2× MIC and incubated at 37°C under mild shaking for 24 hours. Cells were centrifuged, washed three times with PBSt, and fixed by 2.5% paraformaldehyde for 4 hours at 4°C. The pellets were post-fixed in 2% OsO_4 for 30 min and solidified in gelatine. The gelatine blocks were trimmed, gradient-dehydrated, infiltrated, and embedded in resin. Sectioning was performed using ultramicrotome (Leica UCT), and sections (100 nm thick) were stained with lead

citrate before TEM viewing (JEOL 1400Flash).

The aggregation assay was conducted following a published protocol with minor modifications (*76*). Log phase Mab cells were adjusted to OD_{600nm} of 0.25 in 5 ml of 7H9t, and COE-PNH_2 at subinhibitory concentrations were added and incubated under mild shaking for 24 hours. Samples were briefly mixed and left still in an upright position for 10 min. Supernatant was carefully removed without disturbing the pellet settled at the bottom. The OD_{600nm} of the supernatant was recorded as $OD_{supernatant}$. The pellet was resuspended in 5 ml of 7H9t and thoroughly mixed, and the OD_{600nm} was recorded as OD_{pellet}. The aggregation index was calculated as $OD_{pellet}/OD_{supernatant}$, and the plot was normalized to untreated control.

Adhesion assays were conducted in 7H9 medium (without tween 80) following published protocols (*77*). Log phase Mab cells were adjusted to OD_{600nm} of 0.01 and added at 200 µl in 96-well plates. COE-PNH_2 at subinhibitory concentrations were added, and the plate was incubated without agitation at 37°C for 7 days. The supernatant was carefully removed, and wells were washed with PBS for three times to remove unattached bacteria. Crystal violet solution (0.5%) was added to each well and incubated for 15 min to stain the adhered cells. The solution was then discarded, and wells were washed three times to remove excess crystal violet. Acetic acid (30%) was added to dissolve the crystal violet, and the OD_{590nm} was recorded.

To measure intracellular ATP, BacTiter Glo was used following the manufacturer's protocol. Log phase Mab cells were adjusted to OD_{600nm} of 0.05 and added to a 96-well plate at a volume of 200 µl per well. COE-PNH_2 or bedaquiline was added at desired concentrations. The plates were incubated at 37°C under mild shaking for 5 hours. The plates were mixed well, and 50 µl of the suspension in each well was transferred to a white 96-well plate. Freshly prepared BacTiter Glo working solution (50 µl) was added to each well and incubated for 10 min. The bioluminescence was recorded using Tecan Plate reader (Infinite 200 Pro).

To image the ATP-deprived cells from COE-PNH_2 treatment, Mab treated with 1× MIC COE-PNH_2 or PBS vehicle control was washed and stained with Nile Red for 30 min at 37°C. The cells were immobilized in agarose gel and imaged using a fluorescent microscope (Leica Thunder system). To elucidate the ultrastructure of the ILIs, COE-PNH_2–treated cells were washed and fixed by 2.5% paraformaldehyde for 4 hours at 4°C, followed by pellet processing and TEM viewing. ImageJ was used for image processing and quantitative analysis.

In vivo studies

All in vivo studies followed the IACUC guidelines of National University of Singapore (NUS) under approved protocol no. R20-1178. A 5- to 7-week-old female mice were used in all experiments (n = 3 mice per group). ICR mice were purchased from InVivos. C3HeB/FeJ mice were purchased from the Jackson Laboratory and imported via Comparative Medicine Department NUS. Mice were housed in a 12-hour light cycle with free supply of food and water. All animals were acclimated for at least 72 hours before experiments and were randomly assigned to groups.

In vivo efficacy against lung infection

C3HeB/FeJ mice were used to study efficacy. Mice received daily subcutaneous dexamethasone injection at 5 mg/kg as immunosuppressant for 7 days before infection and continued daily throughout the test period. Day of infection is marked as t = 0. Log phase culture of Mab ATCC19977 was washed into PBSt, and OD_{600nm} was adjusted to 0.5. Immediately before infection, bacteria suspension was passed through 27-gauge syringe 10 times to disperse large bacteria clumps. Mice were anesthetized by isoflurane, and bacteria was inoculated intranasally (40 µl per mice). On day 1, one group of mice was euthanized to establish the baseline CFU before treatment. The remaining mice received saline vehicle control daily, COE-PNH_2 treatment every other day (QOD), or daily AMK. All treatments were given intratracheally. Harvesting of mouse organs was done on days 4, 8, and 12, respectively. Lung samples were homogenized, serially diluted, and enumerated by plating onto 7H11 agar plates.

For histopathology, organs were aseptically collected at the experimental end point and incubated in 10% neutral-buffered formalin solution for 48 hours. The fixed samples were submitted for histology evaluation at the Histopathology/Advanced Molecular Pathology Laboratory (AMPL) Agency for Science Technology and Research, following standardized processing (Ziehl-Neelsen stain).

Statistical analysis

Statistical significance was analyzed using one-way analysis of variance (ANOVA) followed by Dunnett's test (GraphPad Prism). *P < 0.05 was considered significant.

Supplementary Materials

This PDF file includes:

scitranslmed.adi7558_sm.pdf

Materials and Methods

Figs. S1 to S13

Tables S1 to S7

Reference (*78*)

adi7558_SupplementalMaterial.docx

Supplementary File_updated

Other Supplementary Material for this manuscript includes the following:

scitranslmed.adi7558_data_file_s1.zip

Data file S1<< Q2 - Query: Insertion of "Data file S1" correct? Ans: **kevin.pethe@ntu.edu.sg:**

A new Data file S1 is uploaded. >>

scitranslmed.adi7558_mdar_reproducibility_checklist.pdf

MDAR Reproducibility Checklist

adi7558_Data_file_S1.xlsx

Data file S1_updated

REFERENCES AND NOTES

1 << Q3 - Query: References 24 and 70 were identical; thus, Ref. 70 was deleted and citations were renumbered accordingly. Please check renumbering. Ans: **kevin.pethe@ntu.edu.sg:** The re-numbering is correct. The reference number in Supplementary Information file is also updated accordingly. >>C. N. Ratnatunga, V. P. Lutzky, A. Kupz, D. L. Doolan, D. W. Reid, M. Field, S. C. Bell, R. M. Thomson, J. J. Miles, The Rise of non-

tuberculosis mycobacterial lung disease. Front. Immunol. 11, 303 (2020).

2 H. Lee, W. Myung, W. J. Koh, S. M. Moon, B. W. Jhun, Epidemiology of nontuberculous mycobacterial infection, South Korea, 2007-2016. Emerg. Infect. Dis. 25, 569–572 (2019).

3 M. M. Johnson, J. A. Odell, Nontuberculous mycobacterial pulmonary infections. J. Thorac. Dis. 6, 210–220 (2014).

4 K. L. Winthrop, T. K. Marras, J. Adjemian, H. Zhang, P. Wang, Q. Zhang, Incidence and prevalence of nontuberculous mycobacterial lung disease in a large U.S. Managed Care Health Plan, 2008–2015. Ann. Am. Thorac. Soc. 17, 178–185 (2020).

5 M.-R. Lee, W.-H. Sheng, C.-C. Hung, C.-J. Yu, L.-N. Lee, P.-R. Hsueh, Mycobacterium abscessus complex infections in humans. Emerg. Infect. Dis. 21, 1638 (2015).

6 M. D. Johansen, J.-L. Herrmann, L. Kremer, Non-tuberculous mycobacteria and the rise of Mycobacterium abscessus. Nat. Rev. Microbiol. 18, 392–407 (2020).

7 V. N. Dahl, M. Mølhave, A. Fløe, J. van Ingen, T. Schön, T. Lillebaek, A. B. Andersen, C. Wejse, Global trends of pulmonary infections with nontuberculous mycobacteria: a systematic review. Int. J. Infect. Dis. 125, 120–131 (2022).

8 J. E. Stout, K. V. Dicks, Calculating the economic benefits of what didn't happen. Int. J. Tuberc. Lung Dis. 20, 854 (2016).

9 M. Mehta, T. K. Marras, Impaired health-related quality of life in pulmonary nontuberculous mycobacterial disease. Respir. Med. 105, 1718–1725 (2011).

10 T. K. Marras, M. A. Campitelli, H. Lu, H. Chung, S. K. Brode, A. Marchand-Austin, K. L. Winthrop, A. S. Gershon, J. C. Kwong, F. B. Jamieson, Pulmonary nontuberculous mycobacteria–associated deaths, Ontario, Canada, 2001–2013. Emerg. Infect. Dis. 23, 468–476 (2017).

11 G. J. Ballarino, K. N. Olivier, R. J. Claypool, S. M. Holland, D. R. Prevots, Pulmonary nontuberculous mycobacterial infections: Antibiotic treatment and associated costs. Respir. Med. 103, 1448–1455 (2009).

12 A. Leber, T. Marras, The cost of medical management of pulmonary nontuberculous mycobacterial disease in Ontario, Canada. Eur. Respir. J. 37, 1158–1165 (2011).

13 C. Cortesia, G. J. Lopez, J. H. de Waard, H. E. Takiff, The use of quaternary ammonium disinfectants selects for persisters at high frequency from some species of non-tuberculous mycobacteria and may be associated with outbreaks of soft tissue infections. J. Antimicrob. Chemother. 65, 2574–2581 (2010).

14 R. Thomson, C. Tolson, H. Sidjabat, F. Huygens, M. Hargreaves, Mycobacterium abscessus isolated from municipal water-a potential source of human infection. BMC Infect. Dis. 13, 1–7 (2013).

15 J. O. Falkinham, Ecology of Nontuberculous Mycobacteria. Microorganisms 9, 2262 (2021).

16 R. C. Lopeman, J. Harrison, M. Desai, J. A. Cox, Mycobacterium abscessus: Environmental bacterium turned clinical nightmare. Microorganisms 7, 90 (2019).

17 R. Nessar, E. Cambau, J. M. Reyrat, A. Murray, B. Gicquel, Mycobacterium abscessus: A new antibiotic nightmare. J. Antimicrob. Chemother. 67, 810–818 (2012).

18 B. E. Ferro, J. van Ingen, M. Wattenberg, D. van Soolingen, J. W. Mouton, Time-kill kinetics of antibiotics active against rapidly growing mycobacteria. J. Antimicrob. Chemother. 70, 811–817 (2015).

19 Y.-K. Yam, N. Alvarez, M.-L. Go, T. Dick, Extreme drug tolerance of Mycobacterium abscessus “persisters”. Front. Microbiol. 11, 359 (2020).

20 A.-L. Roux, A. Viljoen, A. Bah, R. Simeone, A. Bernut, L. Laencina, T. Deramaudt, M. Rottman, J.-L. Gaillard, L. Majlessi, The distinct fate of smooth and rough *Mycobacterium abscessus* variants inside macrophages. Open Biol. 6, 160185 (2016).

21 C. S. Haworth, J. Banks, T. Capstick, A. J. Fisher, T. Gorsuch, I. F. Laurenson, A. Leitch, M. R. Loebinger, H. J. Milburn, M. Nightingale, P. Ormerod, D. Shingadia, D. Smith, N. Whitehead, R. Wilson, R. A. Floto, British Thoracic Society guidelines for the management of non-tuberculous mycobacterial pulmonary disease (NTM-PD). Thorax 72, ii1-ii64 (2017).

22 C. L. Daley, J. M. Iaccarino, C. Lange, E. Cambau, R. J. Wallace Jr., C. Andrejak, E. C. Böttger, J. Brozek, D. E. Griffith, L. Guglielmetti, G. A. Huitt, S. L. Knight, P. Leitman, T. K. Marras, K. N. Olivier, M. Santin, J. E. Stout, E. Tortoli, J. van Ingen, D. Wagner, K. L. Winthrop, Treatment of Nontuberculous mycobacterial pulmonary disease: An official ATS/ERS/ESCMID/IDSA clinical practice guideline. Clin. Infect. Dis. 71, e1–e36 (2020).

23 M.-L. Wu, D. B. Aziz, V. Dartois, T. Dick, NTM drug discovery: Status, gaps and the way forward. Drug Discov. Today 23, 1502–1519 (2018).

24 J. Chen, L. Zhao, Y. Mao, M. Ye, Q. Guo, Y. Zhang, L. Xu, Z. Zhang, B. Li, H. Chu, Clinical efficacy and adverse effects of antibiotics used to treat Mycobacterium abscessus pulmonary disease. Front. Microbiol. 10, 1977 (2019).

25 D. E. Griffith, T. Aksamit, B. A. Brown-Elliott, A. Catanzaro, C. Daley, F. Gordin, S. M. Holland, R. Horsburgh, G. Huitt, M. F. Iademarco, M. Iseman, K. Olivier, S. Ruoss, C. F.

von Reyn, R. J. Wallace, K. Winthrop, A. M. D. Subcommittee, An official ATS/IDSA statement: Diagnosis, treatment, and prevention of nontuberculous mycobacterial diseases. Am. J. Respir. Crit. Care Med. 175, 367–416 (2007).

26 H. Choi, S.-Y. Kim, D. H. Kim, H. J. Huh, C.-S. Ki, N. Y. Lee, S.-H. Lee, S. Shin, S. J. Shin, C. L. Daley, Clinical characteristics and treatment outcomes of patients with acquired macrolide-resistant Mycobacterium abscessus lung disease. Antimicrob. Agents Chemother. 61, e01146–e01117 (2017).

27 J. O. Falkinham III, Challenges of NTM drug development. Front. Microbiol. 9, 1613 (2018).

28 A. Egorova, M. Jackson, V. Gavrilyuk, V. Makarov, Pipeline of anti-Mycobacterium abscessus small molecules: Repurposable drugs and promising novel chemical entities. Med. Res. Rev. 41, 2350–2387 (2021).

29 J. J. Malin, S. Winter, E. van Gumpel, G. Plum, J. Rybniker, Extremely low hit rate in a diverse chemical drug screen targeting mycobacterium abscessus. Antimicrob. Agents Chemother. 63, e01008–e01019 (2019).

30 L. L. Silver, Challenges of antibacterial discovery. Clin. Microbiol. Rev. 24, 71–109 (2011).

31 N. Q. Balaban, S. Helaine, K. Lewis, M. Ackermann, B. Aldridge, D. I. Andersson, M. P. Brynildsen, D. Bumann, A. Camilli, J. J. Collins, C. Dehio, S. Fortune, J.-M. Ghigo, W.-D. Hardt, A. Harms, M. Heinemann, D. T. Hung, U. Jenal, B. R. Levin, J. Michiels, G. Storz, M.-W. Tan, T. Tenson, L. Van Melderen, A. Zinkernagel, Definitions and guidelines for research on antibiotic persistence. Nat. Rev. Microbiol. 17, 441–448 (2019).

32 C. Zhou, G. W. N. Chia, J. C. S. Ho, T. Seviour, T. Sailov, B. Liedberg, S. Kjelleberg, J. Hinks, G. C. Bazan, Informed molecular design of conjugated oligoelectrolytes to increase cell affinity and antimicrobial activity. Angew. Chem. Int. Ed. 57, 8069–8072 (2018).

33 H. Yan, Z. D. Rengert, A. W. Thomas, C. Rehermann, J. Hinks, G. C. Bazan, Influence of molecular structure on the antimicrobial function of phenylenevinylene conjugated oligoelectrolytes. Chem. Sci. 7, 5714–5722 (2016).

34 J. Limwongyut, C. Nie, A. S. Moreland, G. C. Bazan, Molecular design of antimicrobial conjugated oligoelectrolytes with enhanced selectivity toward bacterial cells. Chem. Sci. 11, 8138–8144 (2020).

35 A. Tiihonen, S. J. Cox-Vazquez, Q. Liang, M. Ragab, Z. Ren, N. T. P. Hartono, Z. Liu, S. Sun, C. Zhou, N. C. Incandela, J. Limwongyut, A. S. Moreland, S. Jayavelu, G. C.

Bazan, T. Buonassisi, Predicting antimicrobial activity of conjugated oligoelectrolyte molecules via machine learning. J. Am. Chem. Soc. 143, 18917–18931 (2021).

36 J. Limwongyut, A. S. Moreland, C. Nie, J. Read de Alaniz, G. C. Bazan, Amide moieties modulate the antimicrobial activities of conjugated oligoelectrolytes against Gram-negative bacteria. ChemistryOpen 11, e202100260 (2022).

37 J. M. Belardinelli, D. Verma, W. Li, C. Avanzi, C. J. Wiersma, J. T. Williams, B. K. Johnson, M. Zimmerman, N. Whittel, B. Angala, H. Wang, V. Jones, V. Dartois, V. C. N. de Moura, M. Gonzalez-Juarrero, C. Pearce, A. R. Schenkel, K. C. Malcolm, J. A. Nick, S. A. Charman, T. N. C. Wells, B. K. Podell, J. L. Vennerstrom, D. J. Ordway, R. B. Abramovitch, M. Jackson, Therapeutic efficacy of antimalarial drugs targeting DosRS signaling in *Mycobacterium abscessus*. Sci. Transl. Med. 14, eabj3860 (2022).

38 A. K. Nussbaumer-Pröll, S. Knotzer, S. Eberl, B. Reiter, T. Stimpfl, W. Jäger, S. Poschner, M. Zeitlinger, Impact of erythrocytes on bacterial growth and antimicrobial activity of selected antibiotics. Eur. J. Clin. Microbiol. 38, 485–495 (2019).

39 D. L. Lewis, M. Arens, Resistance of microorganisms to disinfection in dental and medical devices. Nat. Med. 1, 956–958 (1995).

40 G. Fanali, A. Di Masi, V. Trezza, M. Marino, M. Fasano, P. Ascenzi, Human serum albumin: From bench to bedside. Mol. Aspects Med. 33, 209–290 (2012).

41 D. Nagarajan, N. Roy, O. Kulkarni, N. Nanajkar, A. Datey, S. Ravichandran, C. Thakur, I. V. Aprameya, S. P. Sarma, D. Chakravortty, Ω76: A designed antimicrobial peptide to combat carbapenem-and tigecycline-resistant Acinetobacter baumannii. Sci. Adv. 5, eaax1946 (2019).

42 J. Zhang, F. Leifer, S. Rose, D. Y. Chun, J. Thaisz, T. Herr, M. Nashed, J. Joseph, W. R. Perkins, K. DiPetrillo, Amikacin liposome inhalation suspension (ALIS) penetrates non-tuberculous mycobacterial biofilms and enhances amikacin uptake into macrophages. Front. Microbiol. 9, 915 (2018).

43 C. Zhou, Z. Li, Z. Zhu, G. W. Chia, A. Mikhailovsky, R. J. Vázquez, S. J. Chan, K. Li, B. Liu, G. C. Bazan, Conjugated oligoelectrolytes for long-term tumor tracking with incremental NIR-II emission. Adv. Mater. 34, e2201989 (2022).

44 J.-Y. Zhu, G. C. Bazan, Molecular orientation and optimization of membrane dyes based on conjugated oligoelectrolytes. Cell Rep. Phys. Sci. 4, 101429 (2023).

45 J. A. Dykens, Y. Will, The significance of mitochondrial toxicity testing in drug development. Drug Discov. Today 12, 777–785 (2007).

46 P. Rana, M. D. Aleo, M. Gosink, Y. Will, Evaluation of in vitro mitochondrial toxicity

assays and physicochemical properties for prediction of organ toxicity using 228 pharmaceutical drugs. Chem. Res. Toxicol. 32, 156–167 (2018).

47 A. I. Mot, J. R. Liddell, A. R. White, P. J. Crouch, Circumventing the Crabtree Effect: A method to induce lactate consumption and increase oxidative phosphorylation in cell culture. Int. J. Biochem. Cell Biol. 79, 128–138 (2016).

48 V. M. Gohil, S. A. Sheth, R. Nilsson, A. P. Wojtovich, J. H. Lee, F. Perocchi, W. Chen, C. B. Clish, C. Ayata, P. S. Brookes, V. K. Mootha, Nutrient-sensitized screening for drugs that shift energy metabolism from mitochondrial respiration to glycolysis. Nat. Biotechnol. 28, 249–255 (2010).

49 S. J. Pidot, J. L. Porter, T. Lister, T. P. Stinear, In vitro activity of SPR719 against *Mycobacterium ulcerans*, *Mycobacterium marinum* and *Mycobacterium chimaera*. PLoS Negl. Trop. Dis. 15, e0009636 (2021).

50 M. A. De Groote, T. C. Jarvis, C. Wong, J. Graham, T. Hoang, C. L. Young, W. Ribble, J. Day, W. Li, M. Jackson, Optimization and lead selection of benzothiazole amide analogs toward a novel antimycobacterial agent. Front. Microbiol. 9, 2231 (2018).

51 C. Dupont, A. Viljoen, F. Dubar, M. Blaise, A. Bernut, A. Pawlik, C. Bouchier, R. Brosch, Y. Guérardel, J. Lelièvre, A new piperidinol derivative targeting mycolic acid transport in *Mycobacterium abscessus*. Mol. Microbiol. 101, 515–529 (2016).

52 A. P. Kozikowski, O. K. Onajole, J. Stec, C. Dupont, A. Viljoen, M. Richard, T. Chaira, S. Lun, W. Bishai, V. S. Raj, Targeting mycolic acid transport by indole-2-carboxamides for the treatment of *Mycobacterium abscessus* infections. J. Med. Chem. 60, 5876–5888 (2017).

53 C. Raynaud, W. Daher, M. D. Johansen, F. Roquet-Banères, M. Blaise, O. K. Onajole, A. P. Kozikowski, J.-L. Herrmann, J. Dziadek, K. Gobis, Active benzimidazole derivatives targeting the MmpL3 transporter in *Mycobacterium abscessus*. ACS Infect. Dis. 6, 324–337 (2019).

54 U. S. Ganapathy, M. Gengenbacher, T. Dick, Epetraborole is active against *Mycobacterium abscessus*. Antimicrob. Agents Chemother. 65, e01156–e01121 (2021).

55 U. S. Ganapathy, R. González del Rio, M. Cacho-Izquierdo, F. Ortega, J. Lelièvre, D. Barros-Aguirre, M. Lindman, V. Dartois, M. Gengenbacher, T. Dick, A leucyl-tRNA synthetase inhibitor with broad-spectrum antimycobacterial activity. Antimicrob. Agents Chemother. 65, e02420–e02420 (2021).

56 D. I. Andersson, D. Hughes, Microbiological effects of sublethal levels of antibiotics. Nat. Rev. Microbiol. 12, 465–478 (2014).

57 G. S. Chilambi, J. Hinks, A. Matysik, X. Zhu, P. Y. Choo, X. Liu, M. B. Chan-Park, G. C. Bazan, K. A. Kline, S. A. Rice, *Enterococcus faecalis* adapts to antimicrobial conjugated oligoelectrolytes by lipid rearrangement and differential expression of membrane stress response genes. Front. Microbiol. 11, 155 (2020).

58 C. Raynaud, W. Daher, F. Roquet-Banères, M. D. Johansen, J. Stec, O. K. Onajole, D. Ordway, A. P. Kozikowski, L. Kremer, Synergistic interactions of Indole-2-carboxamides and β-lactam antibiotics against *Mycobacterium abscessus*. Antimicrob. Agents Chemother. 64, 10.1128/aac.02548-02519 (2020).

59 M. Gengenbacher, S. P. S. Rao, K. Pethe, T. Dick, Nutrient-starved, non-replicating Mycobacterium tuberculosis requires respiration, ATP synthase and isocitrate lyase for maintenance of ATP homeostasis and viability. Microbiology 156, 81–87 (2010).

60 O. Martins, J. Lee, A. Kaushik, N. C. Ammerman, K. E. Dooley, E. L. Nuermberger, In vitro activity of bedaquiline and imipenem against actively growing, nutrient-starved, and intracellular *Mycobacterium abscessus*. Antimicrob. Agents Chemother. 65, e01545–e01521 (2021).

61 P. Santucci, M. D. Johansen, V. Point, I. Poncin, A. Viljoen, J.-F. Cavalier, L. Kremer, S. Canaan, Nitrogen deprivation induces triacylglycerol accumulation, drug tolerance and hypervirulence in mycobacteria. Sci. Rep. 9, 1–15 (2019).

62 A. Viljoen, M. Blaise, C. de Chastellier, L. Kremer, MAB_3551c encodes the primary triacylglycerol synthase involved in lipid accumulation in Mycobacterium abscessus. Mol. Microbiol. 102, 611–627 (2016).

63 S. Vijay, H. T. Hai, D. D. A. Thu, E. Johnson, A. Pielach, N. H. Phu, G. E. Thwaites, N. T. T. Thuong, Ultrastructural analysis of cell envelope and accumulation of lipid inclusions in clinical mycobacterium tuberculosis isolates from sputum, oxidative stress, and iron deficiency. Front. Microbiol. 8, 2681 (2018).

64 J. G. Hurdle, A. J. O'Neill, I. Chopra, R. E. Lee, Targeting bacterial membrane function: an underexploited mechanism for treating persistent infections. Nat. Rev. Microbiol. 9, 62–75 (2011).

65 E. C. Maggioncalda, E. Story-Roller, J. Mylius, P. Illei, R. J. Basaraba, G. Lamichhane, A mouse model of pulmonary Mycobacteroides abscessus infection. Sci. Rep. 10, 3690 (2020).

66 C. J. Murray, K. S. Ikuta, F. Sharara, L. Swetschinski, G. R. Aguilar, A. Gray, C. Han, C. Bisignano, P. Rao, E. Wool, Global burden of bacterial antimicrobial resistance in 2019: A systematic analysis. Lancet 399, 629–655 (2022).

67 F. Boldrin, R. Provvedi, L. Cioetto Mazzabò, G. Segafreddo, R. Manganelli, Tolerance and Persistence to drugs: A main challenge in the fight against *Mycobacterium tuberculosis*. Front. Microbiol. 11, 1924 (2020).

68 F. P. Maurer, V. L. Bruderer, C. Ritter, C. Castelberg, G. V. Bloemberg, E. C. Böttger, Lack of antimicrobial bactericidal activity in *Mycobacterium abscessus*. Antimicrob. Agents Chemother. 58, 3828–3836 (2014).

69 T. Harada, Y. Akiyama, A. Kurashima, H. Nagai, K. Tsuyuguchi, T. Fujii, S. Yano, E. Shigeto, T. Kuraoka, A. Kajiki, Y. Kobashi, Clinical and microbiological differences between *Mycobacterium abscessus* and *Mycobacterium massiliense* lung diseases. J. Clin. Microbiol. 50, 3556–3561 (2012).

70 C. L. Dulberger, E. J. Rubin, C. C. Boutte, The mycobacterial cell envelope—A moving target. Nat. Rev. Microbiol. 18, 47–59 (2020).

71 H. Chen, S. A. Nyantakyi, M. Li, P. Gopal, D. B. Aziz, T. Yang, W. Moreira, M. Gengenbacher, T. Dick, M. L. Go, The mycobacterial membrane: A novel target space for anti-tubercular drugs. Front. Microbiol. 9, 1627 (2018).

72 N. Mookherjee, M. A. Anderson, H. P. Haagsman, D. J. Davidson, Antimicrobial host defence peptides: functions and clinical potential. Nat. Rev. Drug Discov. 19, 311–332 (2020).

73 D. M. Heithoff, S. P. Mahan, L. Barnes, S. A. Leyn, C. X. George, J. E. Zlamal, J. Limwongyut, G. C. Bazan, J. C. Fried, L. N. Fitzgibbons, J. K. House, C. E. Samuel, A. L. Osterman, D. A. Low, M. J. Mahan, A broad-spectrum synthetic antibiotic that does not evoke bacterial resistance. EBioMedicine 89, 104461 (2023).

74 R. Sorayah, M. S. S. Manimekalai, S. J. Shin, W.-J. Koh, G. Grüber, K. Pethe, Naturally-occurring polymorphisms in QcrB are responsible for resistance to telacebec in *Mycobacterium abscessus*. ACS Infect. Dis. 5, 2055–2060 (2019).

75 S. J. Rose, M. E. Neville, R. Gupta, L. E. Bermudez, Delivery of aerosolized liposomal amikacin as a novel approach for the treatment of nontuberculous mycobacteria in an experimental model of pulmonary infection. PLOS ONE 9, e108703 (2014).

76 S.-H. Tsai, G.-H. Shen, C.-H. Lin, J.-R. Liau, H.-C. Lai, S.-T. Hu, Mab_3168c, a putative acetyltransferase, enhances adherence, intracellular survival and antimicrobial resistance of mycobacterium abscessus. PLOS ONE 8, e67563 (2013).

77 S.-H. Tsai, H.-C. Lai, S.-T. Hu, Subinhibitory doses of aminoglycoside antibiotics induce changes in the phenotype of *Mycobacterium abscessus*. Antimicrob. Agents Chemother. 59, 6161–6169 (2015).

78 L. D. Marroquin, J. Hynes, J. A. Dykens, J. D. Jamieson, Y. Will, Circumventing the Crabtree effect: Replacing media glucose with galactose increases susceptibility of HepG2 cells to mitochondrial toxicants. Toxicol. Sci. 97, 539–547 (2007).

Acknowledgments

We thank the Electron Microscopy Unit in National University of Singapore and the team, particularly A. Y. Sim~~. Aik Yong~~, for the support and assistance in the EM work. We appreciate the advice and scientific discussion of A. Blumenthal (University of Queensland). We thank C. J. E. Pee ~~Jia Ern~~ and B. S.~~hi~~ Lee (Nanyang Technological University) for the help with intracellular ATP assay. We thank L. Cui~~. Liang~~ (Singapore-MIT Alliance for Research and Technology) for the help with high-resolution mass spectrometry experiment. This work was supported in part by the National Research Foundation (NRF) Singapore under its Investigatorship Program (project award number NRF-NRFI06-2020-0004).

Funding: This study was funded by a National University of Singapore Start-up grant (to G.C.B.) and National University of Singapore Yong Loo Lin School of Medicine Kickstart Initiative grant NUHSRO/2022/014/Kickstart/12/LOA (to G.C.B.).

Author contributions: K.Z., A.S.M., and G.C.B. conceptualized the research. J.L., A.S.M. synthesized the compounds. K.Z., S.C.J.W., T.J.J.M., Y.S., S.J.S., S.-Y.K., and B.W.J. contributed to data collection, analysis, and interpretation of biological assays. S.C.J.W. performed fluorescent imaging and processed the images. T.J.J.M. performed the aggregation assay. Y.S. contributed to the protocol establishment of animal studies. S.J.S., S.-Y.K., and B.W.J. contributed to the isolation and characterization of clinical isolates and data interpretation. K.P. and G.C.B. supervised the project. K.Z., K.P., and G.C.B. wrote the manuscript. All authors contributed to the review of the manuscript.

Competing interests: G.C.B., A.S.M., and J.L. are inventors on a patent application covering the use of COEs (WO/2019/183381, short COEs and uses thereof). G.C.B., A.S.M., and K.Z. are cofounders of Xiretsa Inc., a company working to develop antibiotics from the anti-infective COE platform. The remaining authors declare that they have no competing interests.

Data and materials availability: All data needed to evaluate the conclusions in the paper are present in the paper and/or the Supplementary Materials. COE-PNH2 is available from G.C.B. under a materials transfer agreement with the National University of Singapore. Raw data are

available in data file S1.

Queries

Q. No	Query Text	Addressed To	User	Role	Response Thread
Q1	Please provide the expanded form of “ICR,” if any.	Author	kevin.pethe@ntu.edu.sg	Author	There is no expanded form of "ICR". It is a technical term itself.
Q2	Insertion of “Data file S1” correct?	Author	kevin.pethe@ntu.edu.sg	Author	A new Data file S1 is uploaded.
Q3	References 24 and 70 were identical; thus, Ref. 70 was deleted and citations were renumbered accordingly. Please check renumbering.	Author	kevin.pethe@ntu.edu.sg	Author	The re-numbering is correct. The reference number in Supplementary Information file is also updated accordingly.